
Assignment X: Hybridisable Discontinuous Galerkin (#8)
1 Write the HDG formulation of the problem

An equivalent strong form can be written over the broken computational domain as:

$$\begin{cases} -\nabla \cdot (\kappa \nabla u) = s & \text{in } \Omega_i, \text{ and for } i = 1, \dots, n_{el}, \\ u = u_D & \text{on } \Gamma_D \\ \mathbf{n} \cdot (\kappa \nabla u) = t & \text{on } \Gamma_N \\ \mathbf{n} \cdot (\kappa \nabla u) + \gamma u = g & \text{on } \Gamma_R \\ \llbracket u \mathbf{n} \rrbracket = \mathbf{0} & \text{on } \Gamma \\ \llbracket \mathbf{n} \cdot \nabla u \rrbracket = 0 & \text{on } \Gamma \end{cases} \quad (1)$$

Where the two last equations correspond to the imposition of the continuity of the primal variable u and the normal fluxes respectively along the internal interface Γ .

The HDG formulation solves the problem in two phases. First, an element-by-element problem is defined with (\mathbf{q}, u) as unknowns defined as:

$$\begin{cases} \nabla \cdot \mathbf{q}_i = s & \text{in } \Omega_i, \\ \mathbf{q}_i + \kappa \nabla u_i = \mathbf{0} & \text{in } \Omega_i, \\ u_i = u_D & \text{on } \partial\Omega_i \cap \Gamma_D, \\ u_i = \hat{u} & \text{on } \partial\Omega_i \setminus \Gamma_D, \end{cases} \quad (2)$$

for $i = 1, \dots, n_{el}$.

Second, a global problem is defined to determine \hat{u} . The imposition of the so-called transmission conditions,:

$$\begin{cases} \llbracket \mathbf{n} \cdot \mathbf{q} \rrbracket = 0 & \text{on } \Gamma \\ \mathbf{n} \cdot \mathbf{q} = -t & \text{on } \Gamma_N \\ \mathbf{n} \cdot \mathbf{q} = \gamma \hat{u} - g & \text{on } \Gamma_R \end{cases} \quad (3)$$

1.1 Weak form

The weak formulation for each element equivalent to (2) is:

$$\begin{aligned} & -(\nabla v, \mathbf{q}_i)_{\Omega_i} + \langle v, \mathbf{n}_i \cdot \hat{\mathbf{q}}_i \rangle_{\partial\Omega_i} = (v, s)_{\Omega_i} \\ & -(\mathbf{w}, \mathbf{q}_i)_{\Omega_i} + \kappa(\nabla \cdot \mathbf{w}, u_i)_{\Omega_i} = \kappa \langle \mathbf{n}_i \cdot \mathbf{w}, u_D \rangle_{\partial\Omega_i \cap \Gamma_D} + \kappa \langle \mathbf{n}_i \cdot \mathbf{w}, \hat{u} \rangle_{\partial\Omega_i \setminus \Gamma_D} \end{aligned} \quad (4)$$

where the numerical traces of the fluxes $\hat{\mathbf{q}}_i$ are defined, element-by-element as:

$$\mathbf{n}_i \cdot \hat{\mathbf{q}}_i := \begin{cases} \mathbf{n}_i \cdot \mathbf{q}_i + \tau_i(u_i - u_D) & \text{on } \partial\Omega_i \cap \Gamma_D \\ \mathbf{n}_i \cdot \mathbf{q}_i + \tau_i(u_i - \hat{u}) & \text{elsewhere} \end{cases} \quad (5)$$

with τ_i being a stabilization parameter.

The weak form of the global problem is defined by $\hat{u} \in \mathcal{M}(\Gamma \cup \Gamma_N \cup \Gamma_R)$ for all $\mu \in \mathcal{M}(\Gamma \cup \Gamma_N \cup \Gamma_R)$ such that:

$$\sum_{n=1}^{n_{el}} \langle \mu, \mathbf{n}_i \cdot \hat{\mathbf{q}}_i \rangle_{\partial\Omega_i \setminus \partial\Omega} + \sum_{n=1}^{n_{el}} \langle \mu, \mathbf{n}_i \cdot \hat{\mathbf{q}}_i + t \rangle_{\partial\Omega_i \cap \Gamma_N} + \sum_{n=1}^{n_{el}} \langle \mu, \mathbf{n}_i \cdot \hat{\mathbf{q}}_i + g - \gamma \hat{u} \rangle_{\partial\Omega_i \cap \Gamma_R} = 0 \quad (6)$$

Replacing (5) into (6) we have:

$$\begin{aligned} \sum_{n=1}^{n_{el}} \{ \langle \mu, \mathbf{n}_i \cdot \mathbf{q}_i \rangle_{\partial\Omega_i \setminus \Gamma_D} + \langle \mu, \tau_i u_i \rangle_{\partial\Omega_i \setminus \Gamma_D} - \langle \mu, \tau_i \hat{u} \rangle_{\partial\Omega_i \setminus \Gamma_D} - \langle \mu, \gamma \hat{u} \rangle_{\partial\Omega_i \cap \Gamma_R} \} \\ = - \sum_{n=1}^{n_{el}} \{ \langle \mu, g \rangle_{\partial\Omega_i \cap \Gamma_R} + \langle \mu, t \rangle_{\partial\Omega_i \cap \Gamma_N} \} \end{aligned} \quad (7)$$

1.2 Spatial discretization

The following discrete finite-element spaces are introduced:

$$\begin{aligned} \mathcal{W}^h(\Omega) &= \{ \mathbf{w} \in [\mathcal{L}_2(\Omega)]^2; w|_{\Omega_i} \in [\mathcal{P}^p(\Omega_i)]^2 \forall \Omega_i \} && \subset \mathcal{W}(\Omega) \\ \mathcal{V}^h(\Omega) &= \{ v \in [\mathcal{L}_2(\Omega)]^2; v|_{\Omega_i} \in \mathcal{P}^p(\Omega_i) \forall \Omega_i \} && \subset \mathcal{V}(\Omega) \\ \mathcal{M}^h(S) &= \{ \mu \in [\mathcal{L}_2(S)]^2; \mu|_{\Gamma_i} \in \mathcal{P}^p(\Gamma_i) \forall \Omega_i \subset S \subset \Gamma \cup \partial\Omega \} && \subset \mathcal{M}(S) \end{aligned} \quad (8)$$

The variables \mathbf{u} , \mathbf{q} , and \hat{u} are approximated as:

$$\mathbf{q} \approx \mathbf{q}^h = \sum_{n=1}^{n_{el}} N_j \mathbf{q}_j \in \mathcal{W}^h \quad (9)$$

$$u \approx u^h = \sum_{n=1}^{n_{el}} N_j u_j \in \mathcal{V}^h \quad (10)$$

$$\hat{u} \approx \hat{u}^h = \sum_{n=1}^{n_{el}} \hat{N}_j \hat{u}_j \in \mathcal{M}^h(\Gamma \cup \Gamma_N \cup \Gamma_R) \text{ or } \mathcal{M}^h(\Gamma) \quad (11)$$

The weak form of the local problem gives rise to the following system of equations for each element:

$$\begin{bmatrix} \mathbf{A}_{\mathbf{u}\mathbf{u}} & \mathbf{A}_{\mathbf{u}\mathbf{q}} \\ \kappa \mathbf{A}_{\mathbf{u}\mathbf{q}}^T & \mathbf{A}_{\mathbf{q}\mathbf{q}} \end{bmatrix}_i \begin{bmatrix} \mathbf{u}_i \\ \mathbf{q}_i \end{bmatrix} = \begin{bmatrix} \mathbf{f}_u \\ \kappa \mathbf{f}_q \end{bmatrix}_i + \begin{bmatrix} \mathbf{A}_{\mathbf{u}\hat{u}} \\ \kappa \mathbf{A}_{\mathbf{q}\hat{u}} \end{bmatrix}_i \hat{\mathbf{u}}_i \quad (12)$$

Applying the interpolation to (7):

$$\sum_{n=1}^{n_{el}} \left\{ \begin{bmatrix} \mathbf{A}_{\mathbf{u}\hat{\mathbf{u}}}^T & \mathbf{A}_{\mathbf{q}\hat{\mathbf{u}}}^T \end{bmatrix}_i \begin{bmatrix} \mathbf{u}_i \\ \mathbf{q}_i \end{bmatrix} + [\mathbf{A}_{\hat{\mathbf{u}}\hat{\mathbf{u}}}]_i \hat{\mathbf{u}}_i + [\mathbf{A}_{\hat{\mathbf{u}}\hat{\mathbf{u}}}^R]_i \hat{\mathbf{u}}_i \right\} = \sum_{n=1}^{n_{el}} \left\{ [\mathbf{f}_{\hat{\mathbf{u}}}]_i + [\mathbf{f}_{\hat{\mathbf{u}}}^R]_i \right\} \quad (13)$$

In the above equation the matrices $\mathbf{A}_{\hat{\mathbf{u}}\hat{\mathbf{u}}}^R$ and $\mathbf{f}_{\hat{\mathbf{u}}}^R$ are associated to the Robin boundary condition of the problem and are defined as:

$$\mathbf{A}_{\hat{\mathbf{u}}\hat{\mathbf{u}}}^R = - \sum_{\partial\Omega_i \cap \Gamma_R} \gamma \sum_{g=1}^{n_{ip}^f} \hat{\mathbf{N}}_n(\xi_g^f) \hat{\mathbf{N}}^T(\xi_g^f) w_g^f$$

$$\mathbf{f}_{\hat{\mathbf{u}}}^R = - \sum_{\partial\Omega_i \cap \Gamma_R} \sum_{g=1}^{n_{ip}^f} \mathbf{N}(\xi_g^f) g(\mathbf{x}(\xi_g^f)) w_g^f$$

After substituting the local solution (12) in (13):

$$\hat{\mathbf{K}} \hat{\mathbf{u}} = \hat{\mathbf{f}}$$

with

$$\hat{\mathbf{K}} = \bigwedge_{i=1}^{n_{el}} \begin{bmatrix} \mathbf{A}_{\mathbf{u}\hat{\mathbf{u}}}^T & \mathbf{A}_{\mathbf{q}\hat{\mathbf{u}}}^T \end{bmatrix}_i \begin{bmatrix} \mathbf{A}_{\mathbf{u}\mathbf{u}} & \mathbf{A}_{\mathbf{u}\mathbf{q}} \\ \kappa \mathbf{A}_{\mathbf{u}\mathbf{q}}^T & \mathbf{A}_{\mathbf{q}\mathbf{q}} \end{bmatrix}_i^{-1} \begin{bmatrix} \mathbf{A}_{\mathbf{u}\hat{\mathbf{u}}} \\ \kappa \mathbf{A}_{\mathbf{q}\hat{\mathbf{u}}} \end{bmatrix}_i + [\mathbf{A}_{\hat{\mathbf{u}}\hat{\mathbf{u}}}]_i + [\mathbf{A}_{\hat{\mathbf{u}}\hat{\mathbf{u}}}^R]_i$$

and

$$\hat{\mathbf{f}} = \bigwedge_{i=1}^{n_{el}} [\mathbf{f}_{\hat{\mathbf{u}}}]_i + [\mathbf{f}_{\hat{\mathbf{u}}}^R]_i - \begin{bmatrix} \mathbf{A}_{\mathbf{u}\hat{\mathbf{u}}}^T & \mathbf{A}_{\mathbf{q}\hat{\mathbf{u}}}^T \end{bmatrix}_i \begin{bmatrix} \mathbf{A}_{\mathbf{u}\mathbf{u}} & \mathbf{A}_{\mathbf{u}\mathbf{q}} \\ \kappa \mathbf{A}_{\mathbf{u}\mathbf{q}}^T & \mathbf{A}_{\mathbf{q}\mathbf{q}} \end{bmatrix}_i^{-1} \begin{bmatrix} \mathbf{f}_{\mathbf{u}} \\ \kappa \mathbf{f}_{\mathbf{q}} \end{bmatrix}_i$$

2 Results

Considering:

$$u(x, y) = k \log((x + a)^2) + \cos(b(y - \gamma)^3) \quad (14)$$

With the following data: $k = 1.4, \gamma = 2.2, a = 1$ and, $b = 3$

We can first plot the above function (14), and take it as a reference.

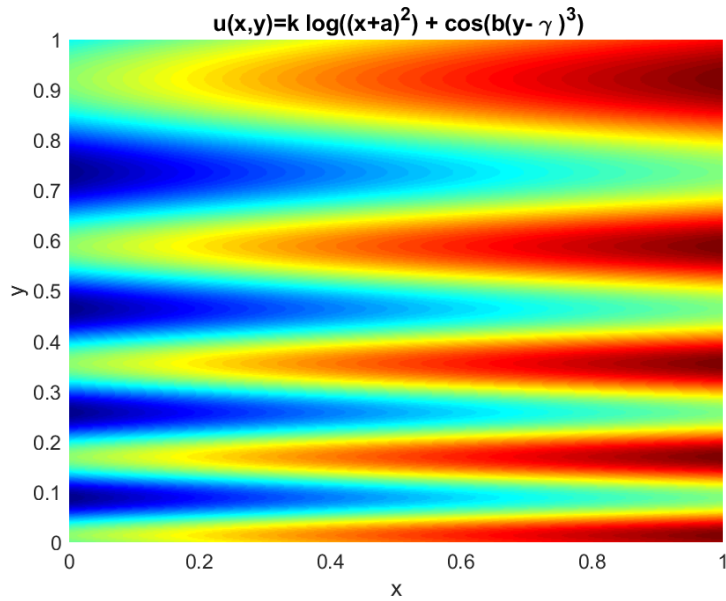


Figure 2.1: Plot of the function

Analytic expression for u_D , t , and g were computed using the MATLAB symbolic tools.

$$u_D = \begin{cases} \frac{7 \ln((x+1)^2)}{5} + 0.8638 & y = 0 \\ \frac{7 \ln((x+1)^2)}{5} + 0.4543 & y = 1 \end{cases}$$

Neumann ($y=0$)

$$t = -30.7280$$

Robin ($y=1$)

$$g = \frac{77 \ln((x+1)^2)}{25} - 15.1638$$

Corresponding expressions were introduced in the existing functions `analyticalPoisson.m` and `sourcePoisson.m` for the computations of the source term and the exact solution, which also includes the computations for the Dirichlet boundary values.

New functions were added for the mathematical expressions for t and g : `neumanPoisson.m` and `robinPoisson.m`, respectively.

Now we have to separate the faces in which we are going to apply the boundary conditions, for this a new function called `ExtFace_class.m` was introduced. This new function divides the external boundary faces into Neumann, Dirichlet and Robin.

First, it is shown for a linear approximation different meshes:

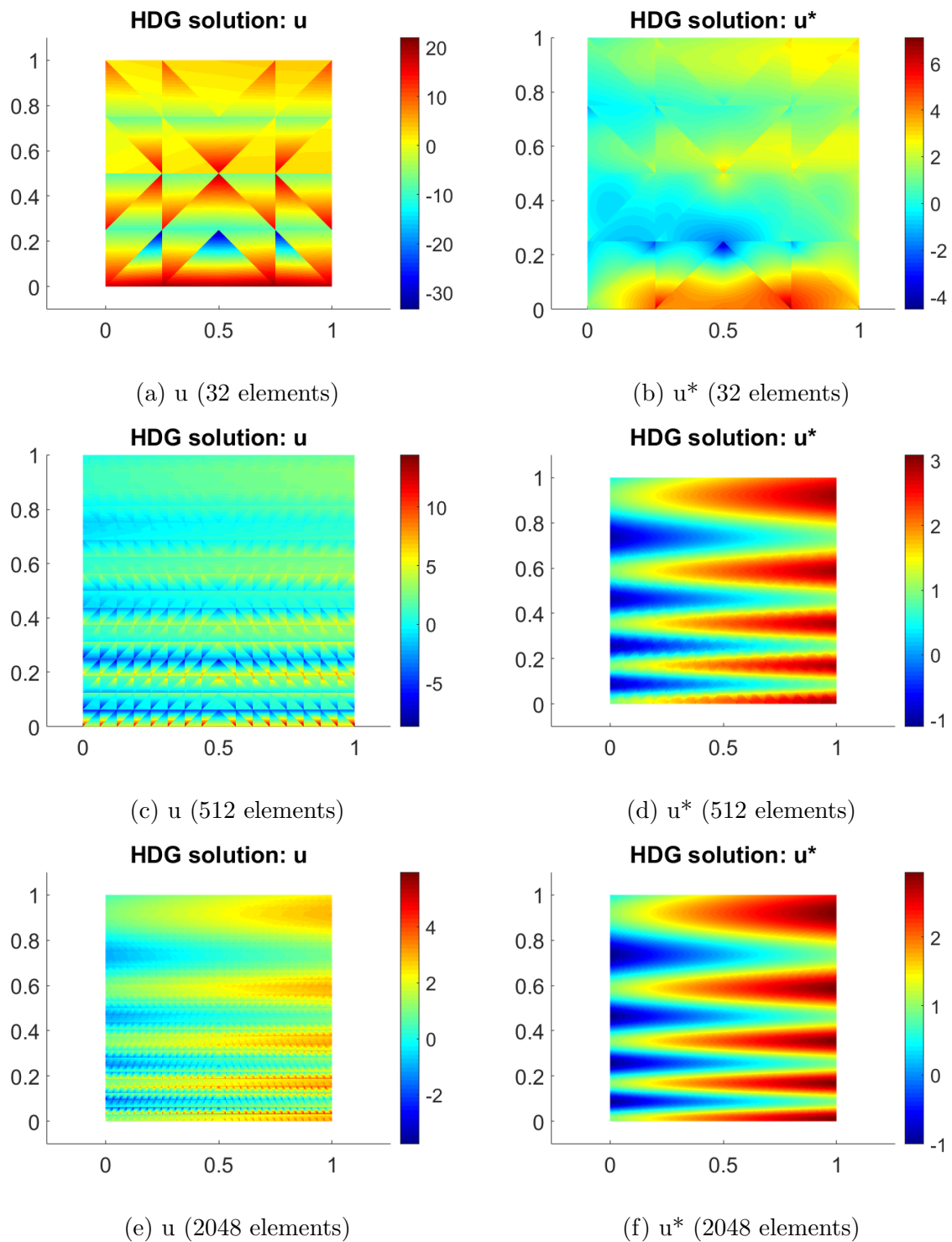


Figure 2.2: Comparison of the solution u and the postprocessed solution u^* using a linear approximation different meshes.

It is possible to observe how, for a greater number of elements, the error decreases. In

the following table we can see it clearly comparing the errors obtained:

	Number of elements		
	32	512	2048
Error u	6.111686e+00	1.335498e+00	3.804581e-01
Error u*	1.199813e+00	3.129223e-02	4.110906e-03

Table 1: Comparison of the error of the solution u and the error of the postprocessed solution u^* using a linear approximation with different meshes.

In the following graphs we compare two meshes used with a approximation polynomial of degree 2:

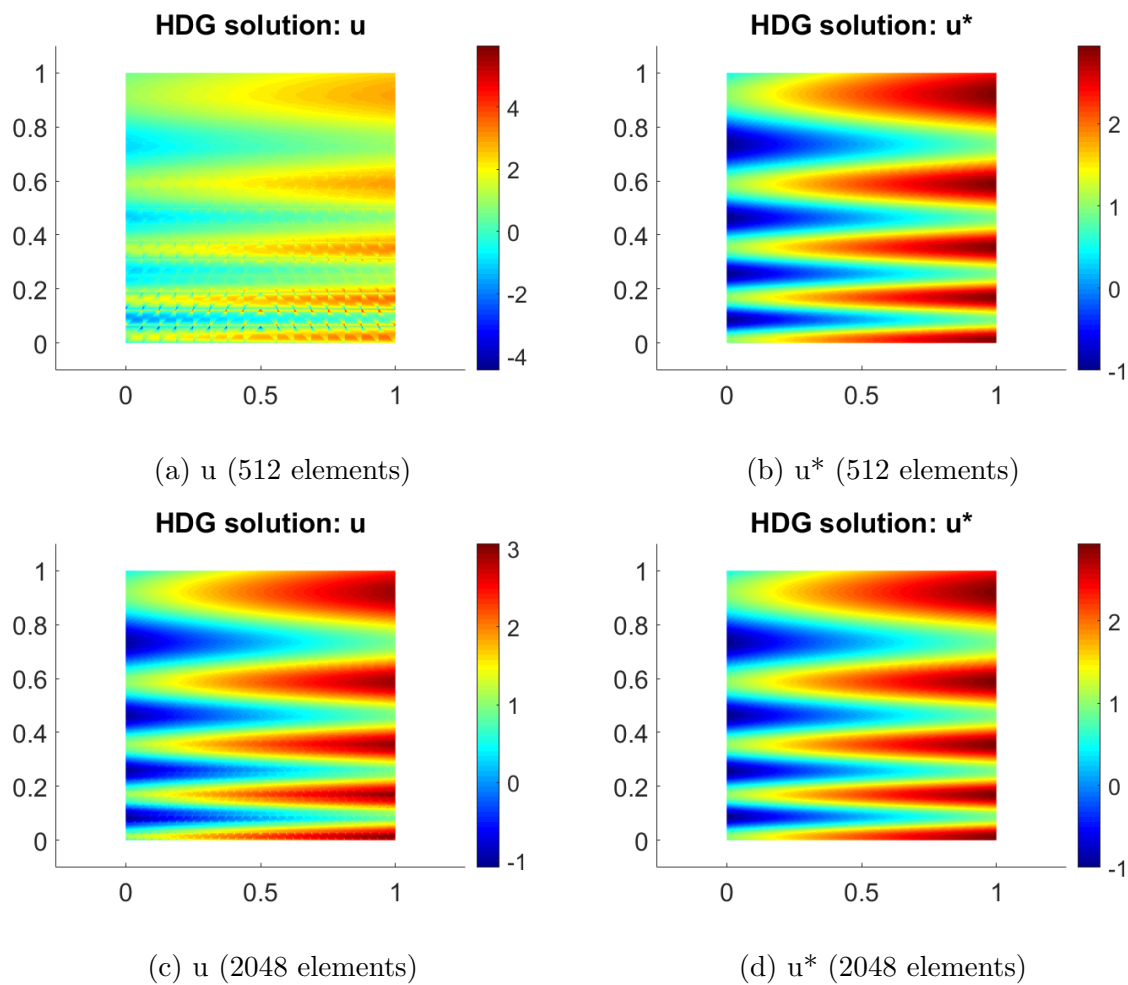


Figure 2.3: Comparison of the solution u and the postprocessed solution u^* using a quadratic approximation different meshes.

In the following table we can see the comparison of the error values for the different types of meshes.

	Number of elements	
	512	2048
Error u	3.055186e-01	4.043895e-02
Error u*	4.084938e-03	2.593626e-04

Table 2: Comparison of the errors of the solution u and the postprocessed solution u^* using a quadratic approximation different meshes.

It is important to note how for 512 elements we have a minor error for a linear approximation in the postprocessed solution and a linear polynomial approximation compared to the solution for 512 elements and quadratic approximation.

In the following graphs, we compared two meshes used with an approximation polynomial of degree 4:

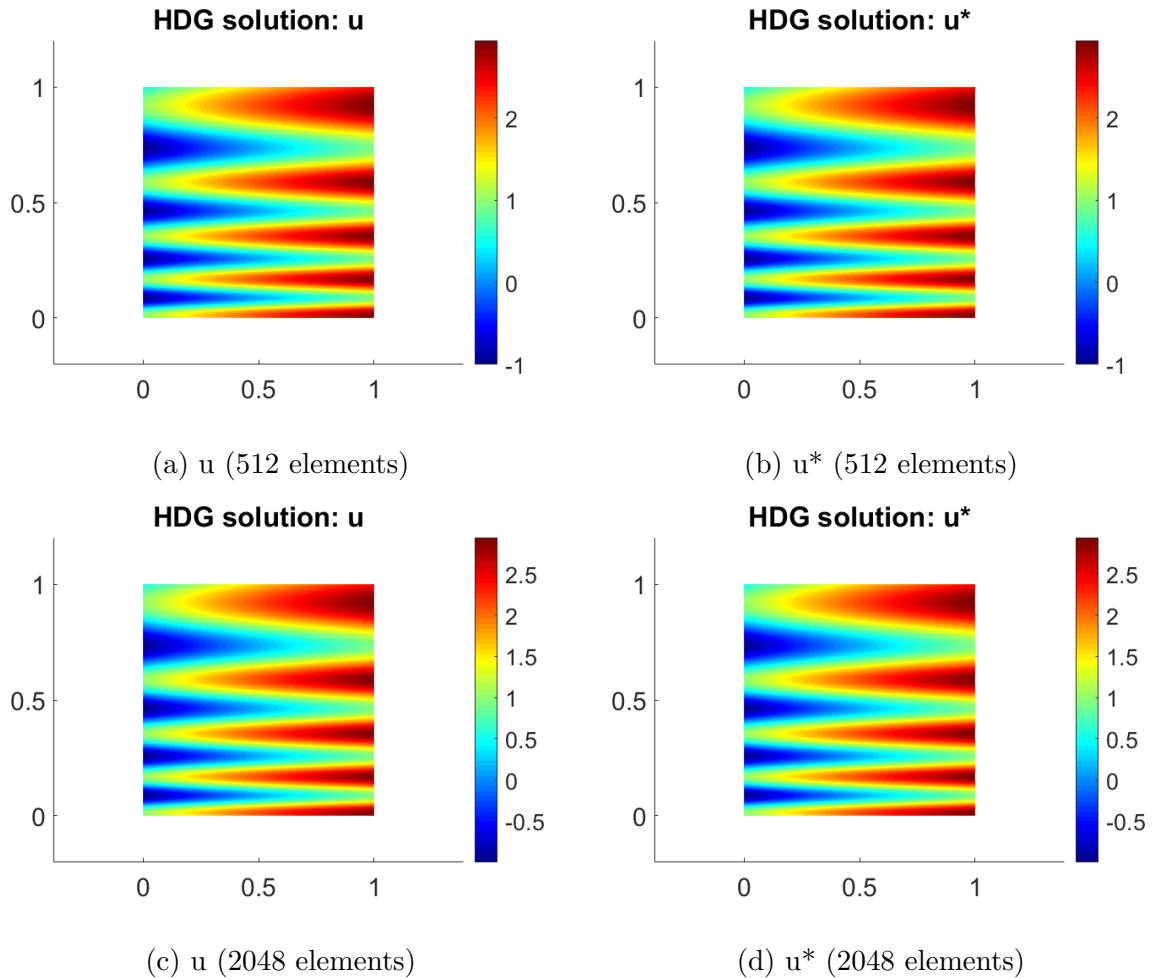


Figure 2.4: Comparison of the solution u and the postprocessed solution u^* using a fourth order polynomial approximation different meshes.

The following table shows the comparison of the error values for the different types of meshes.

	Number of elements	
	512	2048
Error u	5.356439e-03	1.946896e-04
Error u*	4.258941e-05	7.506174e-07

Table 3: Comparison of the errors of the solution u and the postprocessed solution u^* using a fourth order polynomial approximation different meshes.

An h-convergence study of the error of solution and the post-processed solution is performed.

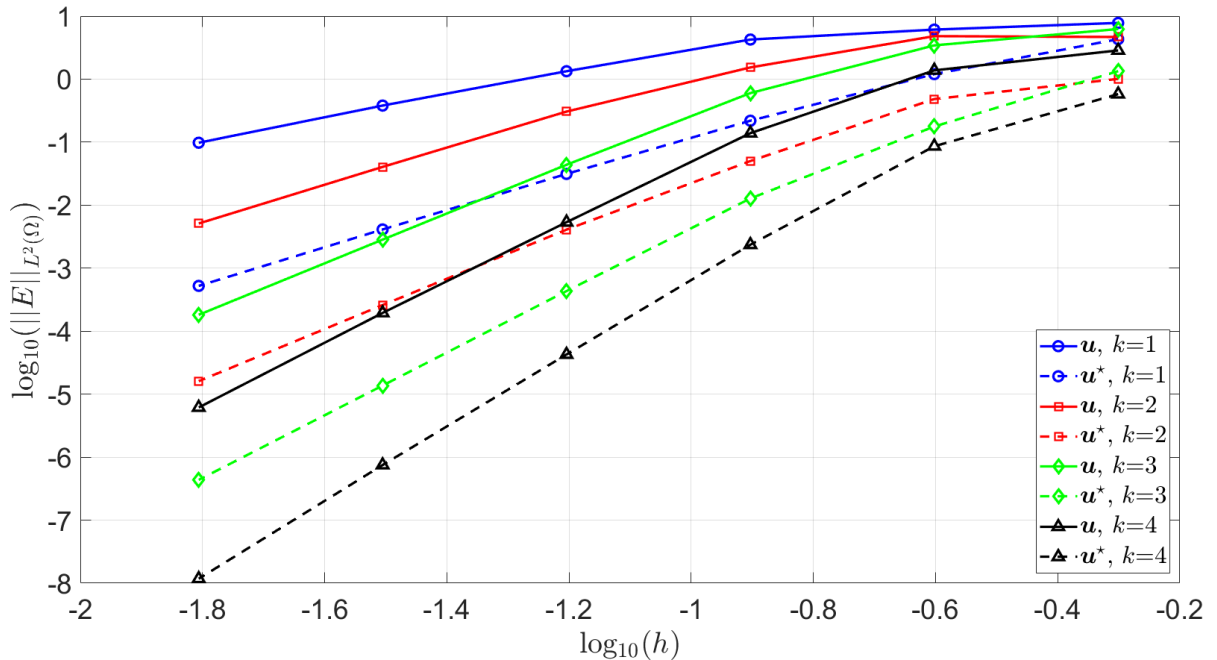


Figure 2.5: Error of the solution and the post-processed solution in the $\mathcal{L}_2(\Omega)$ norm as a function of the characteristic element size h for different values of the approximation degree p

The colors represent the polynomial degree. As can be seen as the number of elements in the mesh increases, the error decreases. Something very important to emphasize are the improvements of the HDG methodology in the postprocess computation, where the solution u^* that is shown with dashed lines gains precision.